

# Hierarchical Supramolecular Assembly of Sterically Demanding $\pi$ -Systems by Conjugation with Oligoprolines\*\*

Urszula Lewandowska, Wojciech Zajaczkowski, Long Chen, Francelin Bouillière, Dapeng Wang, Kaloian Koynov, Wojciech Pisula, Klaus Müllen,\* and Helma Wennemers\*

**Abstract:** Self-assembly from flexible worm-like threads via bundles of rigid fibers to nanosheets and nanotubes was achieved by covalent conjugation of perylene monoimide (PMI) chromophores with oligoprolines of increasing length. Whereas the chromophoric  $\pi$ -system and the peptidic building block do not self-aggregate, the covalent conjugates furnish well-ordered supramolecular structures with a common wall/fiber thickness. Their morphology is controlled by the number of repeat units and can be tuned by seemingly subtle structural modifications.

Precise control over the incorporation and ordering of functional building blocks into larger, organized systems is important for the development of new materials.<sup>[1]</sup> As the material properties are ultimately inscribed in the molecular structure of the self-assembling building blocks, strategies to control supramolecular architectures are important.<sup>[2]</sup> Peptides that adopt well-defined secondary structures are attractive for this goal, as they are chemically robust and accessible by modular synthetic routes. Several studies have shown the value of conjugates between  $\pi$ -systems and  $\alpha$ -helical or  $\beta$ -sheet peptides for the development of supramolecular structures. In all of these conjugates, the intrinsic self-assembly properties of the peptides and/or the  $\pi$ -systems were used to control the supramolecular architecture.<sup>[3,4]</sup>

Herein, we explored the self-assembly of conjugates between building blocks that do not self-assemble on their own but within which the peptidic scaffold serves to control the number and the spatial orientation of the  $\pi$ -systems relative to each other. We chose oligoprolines as peptidic scaffolds and alkynylated perylene monoimides (PMIs) bearing sterically demanding isopropyl groups, which are known to obstruct the  $\pi$ -stacking of PMIs, as chromophores

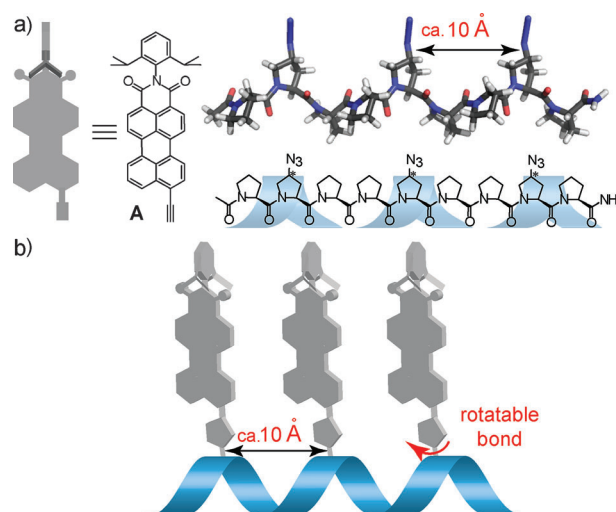


**Figure 1.** Oligoproline- $\pi$ -system conjugates. a) Left: alkynylated PMI bearing isopropyl groups (**A**), right: model of an oligoproline PPII-helix with Azp residues in every third position. b) Representation of a conjugate.

(Figure 1).<sup>[5]</sup> Oligoprolines are highly symmetric helical peptides that have no tendency to self-aggregate but allow, by incorporation of (4*S*)- or (4*R*)-azidoproline (Azp) residues, for functionalization with  $\pi$ -systems at well-defined distances.<sup>[5]</sup> They adopt already at short chain lengths of six proline residues the conformationally well-defined left-handed polyproline II (PPII) helix, in which every third residue is stacked on top of each other in a distance of about 10 Å (Figure 1 a).<sup>[6]</sup> Furthermore, they allow for the facile and modular synthesis of conjugates with desired lengths and are known for their good solubility in both aqueous and organic solvents. These features render oligoprolines ideal scaffolds for probing whether control over the number and spatial preorganization of  $\pi$ -systems suffices for the formation of well-defined supramolecular structures.<sup>[6,7]</sup>

Herein, we show that conjugation of oligoprolines with PMI **A** leads to the formation of hierarchical supramolecular assemblies with tunable properties. With increasing length of the oligoproline- $\pi$ -system conjugates, higher ordered nanostructures form that range from flexible worm-like threads via fibrils to nanosheets and nanoribbons. We also show that the helicity of the chiral aggregates can be reversed by changing the stereochemistry on the outer rim of the oligoproline scaffold while maintaining the stereochemistry within the peptidic backbone.

[\*] Dr. U. Lewandowska, Dr. F. Bouillière, Prof. H. Wennemers  
Laboratory of Organic Chemistry, ETH Zürich  
Vladimir-Prelog-Weg 3, 8093 Zürich (Switzerland)  
E-mail: Helma.Wennemers@org.chem.ethz.ch  
W. Zajaczkowski, Dr. L. Chen, Dr. D. Wang, Dr. K. Koynov,  
Dr. W. Pisula, Prof. K. Müllen  
Max Planck Institute for Polymer Research  
Ackermannweg 10, 55128 Mainz (Germany)  
E-mail: muellen@mpip-mainz.mpg.de

[\*\*] We are grateful for financial support by the VW foundation and support by the Electron Microscopy Center of ETH Zurich (EMEZ). We thank Dr. G. Joshi and Dr. L. Smeenk for assistance with early versions of this manuscript and Prof. F. Diederich and his group for assistance with GPC and acquisition of fluorescence data.

Supporting information for this article is available on the WWW under <http://dx.doi.org/10.1002/anie.201408279>.

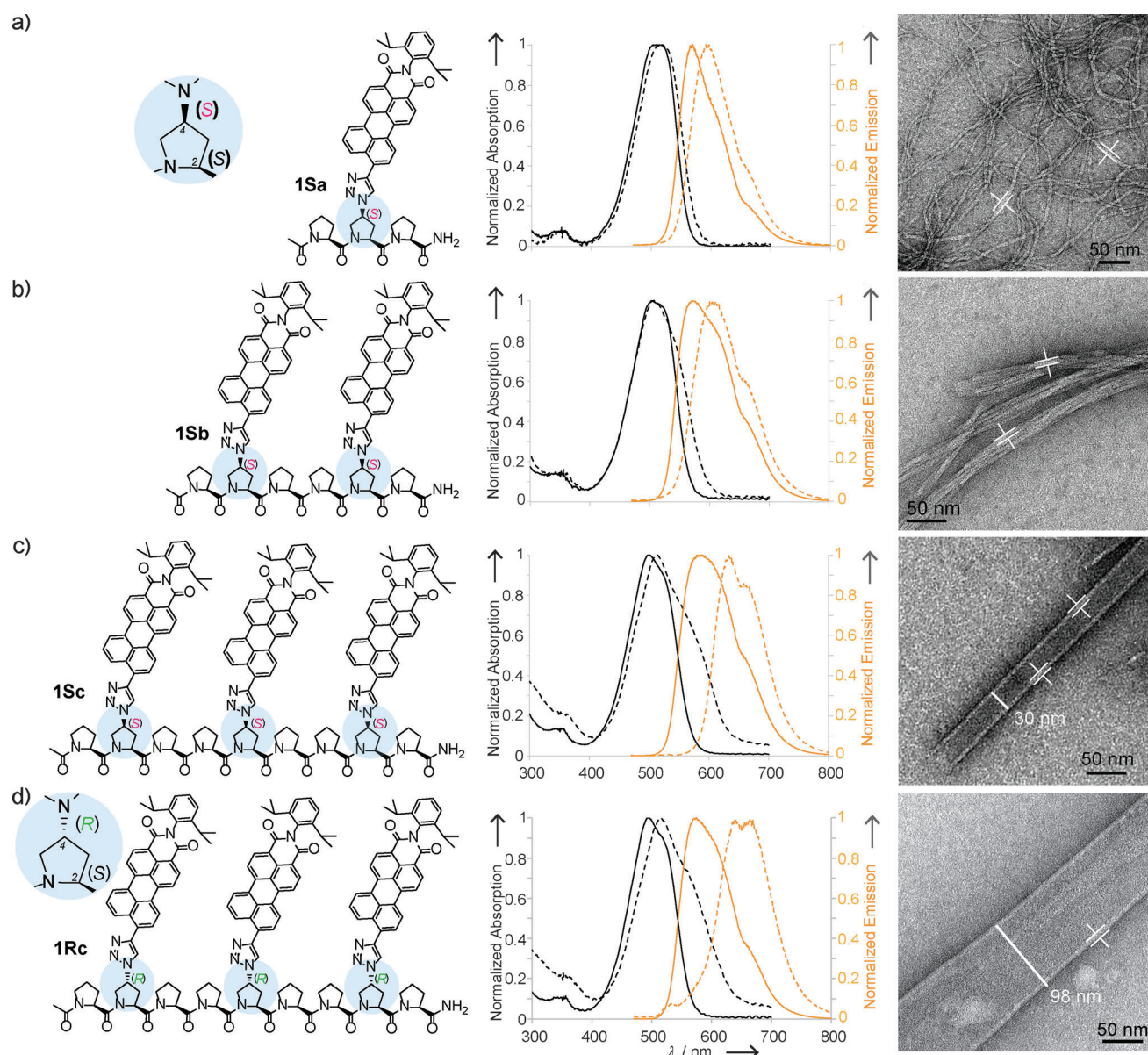


**Figure 2.** Left: Structures of oligoproline-PMI conjugates **1Sa-c** and **1Rc**. Middle: Normalized absorption (black, 50  $\mu$ M at 294 K) and emission (orange, 5  $\mu$ M at 294 K,  $\lambda_{\text{ex}} = 450$  nm) spectra of **1Sa-c** and **1Rc** in 100% THF (solid line) and THF/H<sub>2</sub>O (30:70) (dashed line). Right: TEM micrographs of **1Sa-c** and **1Rc** deposited from THF/H<sub>2</sub>O (30:70) solutions after 7 days of incubation (50  $\mu$ M for **1Sa**, **1Sb** and 5  $\mu$ M for **1Sc** and **1Rc**) and staining with 2% uranyl acetate.

We started by synthesizing conjugates **1Sa**, **1Sb**, and **1Sc** bearing (4*S*)Azp residues as attachment sites for one, two, and three *i*PrPery units, respectively, by a combination of solid phase peptide synthesis and click chemistry (Figure 2, left).<sup>[8,9]</sup> Whereas the oligoproline and the  $\pi$ -systems are conformationally well-preorganized, the connecting bonds between them are rotatable and the only sites with significant degree of conformational freedom within the conjugates (Figure 1b).

The properties of **1Sa-c** were first studied in solutions of THF (50  $\mu$ M) by UV/Vis and fluorescence spectroscopy. The absorption spectra of **1Sa-c** are typical for molecularly dissolved PMIs with  $\lambda_{\text{max abs}}$  at 500  $\pm$  4 nm (Figure 2a-c, middle, black solid lines). The absorption band of the  $\pi$ - $\pi^*$  transition shifted to longer wavelengths when water was

added and reached a maximal shift at a ratio of THF/H<sub>2</sub>O of 30:70 (Figure 2a-c, middle, black dashed lines). Emission spectra of **1Sa-c** showed even more distinct redshifts and the appearance of a low-energy  $\pi$ - $\pi^*$  transition band in THF/H<sub>2</sub>O mixtures (Figure 2, middle, orange lines). The bathochromic shifts were most pronounced for the 9-mer **1Sc** with three PMIs for which a shift of the absorption maximum by 14 nm to  $\lambda_{\text{max abs}} = 514$  nm and of the emission maximum by 44 nm to  $\lambda_{\text{max em}} = 633$  nm was observed (Figure 2c, middle). Such red-shifts are indicative of the formation of J-aggregates within which the planes of the  $\pi$ -systems are not stacked on top of each other but are organized intermolecularly in an offset fashion.<sup>[10]</sup>

Fluorescence correlation spectroscopy (FCS) revealed the critical aggregation concentrations (CAC) of the conjugates **1Sa–c** in THF/H<sub>2</sub>O (30:70) solutions.<sup>[11]</sup> Whereas conjugate **1Sc** aggregated at a concentration of as low as 10 nM, **1Sb** aggregated only at about 1  $\mu$ M, and **1Sa** did not aggregate in the range of concentrations accessible by FCS (1 nM–1  $\mu$ M). Thus, the self-assembly of the conjugates becomes more and more favored with increasing oligoproline–PMI repeat units, which is in agreement with the UV/Vis and fluorescence spectroscopic studies.<sup>[12]</sup>

To explore the generality of the approach we prepared and analyzed the supramolecular assembly properties of oligoproline–PMI conjugate **1Rc** with (4*R*)Azp residues as attachment sites for the PMI (Figure 2d, left). Thus, it is a diastereoisomer of **1Sc** that consists of the same building blocks but differs in the stereochemistry of the carbons at the outside of the oligoproline scaffold. UV/Vis and fluorescence spectra of solutions of **1Rc** in THF and THF/H<sub>2</sub>O (30:70) mixtures are similar to those of **1Sc** (Figure 2d, middle). The observed bathochromic shifts of 20 nm to  $\lambda_{\text{max abs}} = 514$  nm and 64 nm to  $\lambda_{\text{max em}} = 633$  nm, respectively, upon changing the solvent are even larger compared to those observed for **1Sc** and demonstrate that also **1Rc** self-assembles by the formation of J-aggregates.

Transmission electron microscopy (TEM) was then used to investigate the morphology of the supramolecular aggregates. Towards this goal, solutions of **1Sa**, **1Sb**, **1Sc**, and **1Rc** in mixtures of THF and H<sub>2</sub>O (30:70) were deposited on a carbon-coated copper grid and monitored after negatively staining with 2% uranyl acetate. The micrographs revealed distinct nanostructures for each of the peptide–PMI conjugates (Figure 2, right). Whereas the oligoproline trimer **1Sa** with one PMI moiety formed spaghetti-like, entangled networks, a rigidification of the threads into bundles was observed for oligoproline hexamer **1Sb** with two PMIs. An even higher ordered, folded nanoribbon structure was observed for the oligoproline nonamers **1Sc** and **1Rc** with three PMI moieties. This hierarchical self-assembly demonstrates that increasingly ordered supramolecular structures form with increasing length of the oligoproline–PMI conjugates. Remarkably, all of the derivatives have a constant

average fiber/wall thickness of about 5–6 nm. These observations indicate that the common diameter of the supramolecular assemblies is determined by the height of the conjugates, whereas their lengths, that is, the number of repeat units, control the morphology and rigidity of the assemblies. The width of the folded nanosheets formed by **1Rc** are between 50–100 nm (Figure 2d, right), whereas those formed by **1Sc**, the diastereoisomer of **1Rc**, are narrower (30–50 nm). This shows that subtle changes within the molecular structure of the oligoproline scaffold allow for fine-tuning of the supramolecular assembly.<sup>[13]</sup>

To gain deeper insight into the supramolecular organization of the oligoproline–PMI conjugates, grazing-incidence wide-angle X-ray scattering (GIWAXS) was performed with the most highly ordered conjugates **1Rc** and **1Sc** (Figure 3a). The GIWAXS patterns of both conjugates are similar and indicative of similar supramolecular assemblies. However, the observed reflexes for **1Rc** are sharper compared to those of **1Sc**,<sup>[9]</sup> which suggests a higher supramolecular order of **1Rc**. The data revealed wide-angle equatorial scattering intensities that are related to the typical  $\pi$ -stacking distance of 3.40 Å and an intermolecular period of 3.70 Å for tilted or shifted PMI units that undergo the intercalation (B in Figure 3a,c). Thereby, the stacking axis and the tilting vector are oriented in the same plane parallel with respect to the surface. The relation of both distances of 3.40 Å and 3.70 Å implies an in-plane tilting angle of about 23° of the  $\pi$ -stacked PMI cores relative to the axis of the oligoproline scaffold. These reflexes are in agreement with the formation of J-aggregates by a ladder-like arrangement within the nanosheets, which correspond well with the observed J-aggregates by UV/Vis and fluorescence spectroscopy. The additional small-range reflection at  $q_{xy} = 0.28 \text{ Å}^{-1}$  (C in Figure 3a,b) is assigned to the spacing of 22.20 Å, which corresponds to the distance between the first and third PMI unit along the nonapoline, while the middle-range one at  $q_{xy} = 0.78 \text{ Å}^{-1}$  ( $d = 8.06 \text{ Å}$ ) depicts the distance between the oligoproline helices (D in Figure 3a,c).<sup>[14]</sup> The meridional reflections (along  $q_{xy} = 0 \text{ Å}^{-1}$ ) correspond to a d-spacing of 25.00 Å, which is in agreement with an organization of the conjugate into an intercalated double layer (A in Figure 3a,b).<sup>[14]</sup> Within such an organ-

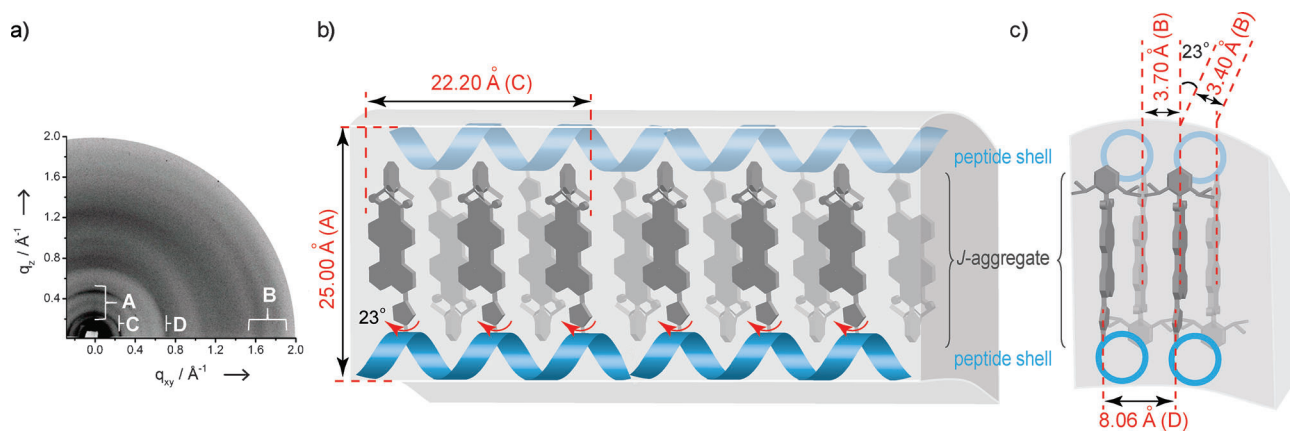


**Figure 3.** a) GIWAXS of **1Rc** after deposition from THF/H<sub>2</sub>O (30:70) solution and 7 days of incubation. b), c) Model of the supramolecular organization of **1Rc**: b) front view; c) side view.



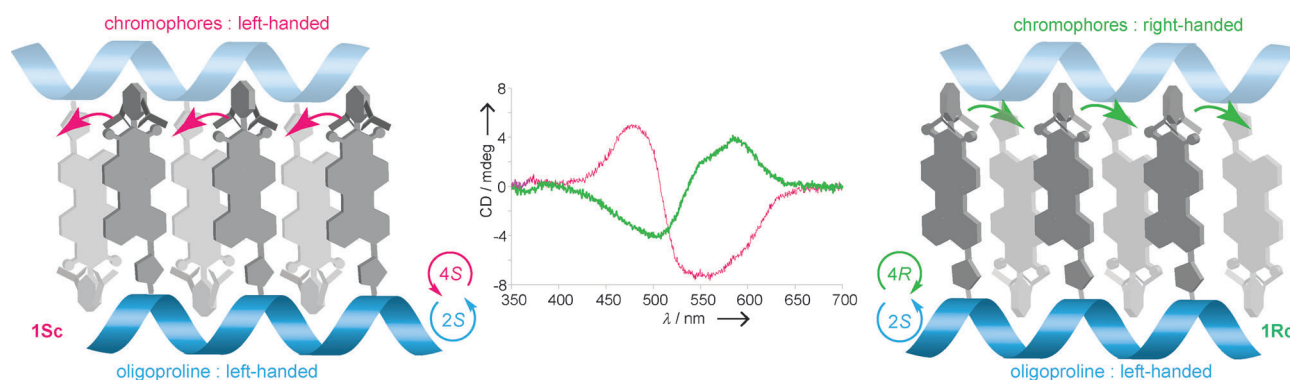


**Figure 4.** CD spectra of diastereoisomers **1Sc** (magenta) and **1Rc** (green) in THF/H<sub>2</sub>O (30:70, 50 μM, 294 K; middle). Representation of the counter-clockwise and clockwise orientation of chromophores within **1Sc** (left) and **1Rc** (right), respectively.

ization, the bulky isopropyl moieties of the PMI fit into the grooves of the oligoproline scaffold and form together with the  $\pi$ -systems a hydrophobic inner part whereas the hydrophilic oligoprolines are at the outside of the assembly. This height of 25.00 Å of the double layer corresponds well with the thickness of the walls of the nanoribbons that were observed for **1Rc** and **1Sc** by TEM since negative staining is known to add a layer of approximately 15–20 Å to the nanostructure.<sup>[15]</sup>

Finally, we investigated whether the oligoproline–PMI conjugates form chiral supramolecular assemblies in solution and recorded circular dichroism (CD) spectra of solutions of **1Sa–c** and **1Rc** in THF/H<sub>2</sub>O (30:70) mixtures. For the oligoproline trimers and hexamers **1Sa** and **1Sb** with one and two PMIs, respectively, no or only weak bisignated CD spectra in the  $\pi$ – $\pi^*$  absorption region were observed, indicating the absence of enantiomerically enriched supramolecular structures.<sup>[9]</sup> In contrast, the CD spectrum of oligoproline nonamer **1Sc** with three PMI moieties showed a distinct negative bisignated Cotton Effect (CE)<sup>[16]</sup> with a zero crossing in the  $\pi$ – $\pi^*$  absorption region at 507 nm (Figure 4, middle, magenta). This is indicative of PMI moieties that aggregate with their transition dipoles oriented in a counter-clockwise helical orientation, the same left-handed helicity as that of the oligoproline PPII backbone (Figure 4, left). Thus, an oligoproline nonamer functionalized with three PMIs suffices for the formation of chiral aggregates. Remarkably, the CD spectrum of **1Rc**, the diastereoisomer of **1Sc**, which differs only in the absolute configuration at C4, but not that at C2 of the oligoproline backbone, showed a bisignated CE with opposite sign compared to that of **1Sc** (Figure 4, green). In fact, this positive bisignated CE with a zero crossing in the  $\pi$ – $\pi^*$  absorption region is almost a mirror image of the spectrum of **1Sc** (Figure 4, middle). Thus, the PMI moieties within **1Rc** form chiral self-assemblies with a clockwise (right-handed) helical orientation, whereas those of **1Sc** orient themselves in a counter-clockwise (left-handed) direction. This is a striking outcome since the absolute configuration of the peptidic backbone is the same within both **1Sc** and **1Rc** (Figure 2c,d).

In summary, we have demonstrated the value of functionalizable peptidic scaffolds that have no tendency to self-aggregate but govern the spatial orientation between  $\pi$ -

systems for directed self-assembly. Easily modifiable parameters within the molecular structure, such as the length of the conjugate and the absolute configuration of stereocenters at the outside of the helix, allowed for tuning the supramolecular aggregation. These features combined with the modularity of the molecular design within which the nature of the chromophores and their spatial arrangement can be varied at will, render oligoproline– $\pi$ -system conjugates a unique and highly modular platform for the further development of tailored functional supramolecular self-assemblies that may be valuable for example in the development of organic field-effect transistors and other devices.

Received: August 15, 2014

Published online: October 10, 2014

**Keywords:** J-aggregates · nanostructures · peptides ·  $\pi$ – $\pi$  interactions · self-assembly

- [1] a) B. D. Gates, Q. Xu, M. Stewart, D. Ryan, C. G. Willson, G. M. Whitesides, *Chem. Rev.* **2005**, *105*, 1171–1196; b) A. C. Grimsdale, K. Müllen, *Angew. Chem. Int. Ed.* **2005**, *44*, 5592–5629; *Angew. Chem.* **2005**, *117*, 5732–5772; c) F. S. Kim, G. Ren, S. A. Jenekhe, *Chem. Mater.* **2011**, *23*, 682–732; d) R. Steyrleuthner, R. Di Pietro, B. A. Collins, F. Polzer, S. Himmelberger, M. Schubert, Z. Chen, S. Zhang, A. Salleo, H. Ade, A. Facchetti, D. Neher, *J. Am. Chem. Soc.* **2014**, *136*, 4245–4256.
- [2] For reviews, see: a) C. C. Lee, C. Grenier, E. W. Meijer, A. P. H. J. Schenning, *Chem. Soc. Rev.* **2009**, *38*, 671–683; b) E. Schwartz, S. Le Gac, J. J. L. M. Cornelissen, R. J. M. Nolte, A. E. Rowan, *Chem. Soc. Rev.* **2010**, *39*, 1576–1599; c) D. Gonzalez-Rodriguez, A. P. H. J. Schenning, *Chem. Mater.* **2011**, *23*, 310–325; d) S. I. Stupp, L. C. Palmer, *Chem. Mater.* **2014**, *26*, 507–518.
- [3] For reviews, see: a) D. N. Woolfson, Z. N. Mahmoud, *Chem. Soc. Rev.* **2010**, *39*, 3464–3479; b) D. W. P. M. Löwik, E. H. P. Leunissen, M. van den Heuvel, M. B. Hansen, J. C. M. van Hest, *Chem. Soc. Rev.* **2010**, *39*, 3394–3412; c) J. D. Tovar, *Acc. Chem. Res.* **2013**, *46*, 1527–1537.
- [4] For examples that use the intermolecular aggregation properties of  $\alpha$ -helical or  $\beta$ -sheet forming peptides to trigger the self-assembly of peptide– $\pi$ -system conjugates into higher ordered structures, see: a) N. Ashkenasy, W. S. Horne, M. R. Ghadiri, *Small* **2006**, *2*, 99–102; b) C. E. Finlayson, R. H. Friend, M. B. J. Otten, E. Schwartz, J. J. L. M. Cornelissen, R. J. M. Nolte, A. E.

- Rowan, P. Samori, V. Palermo, A. Liscio, K. Peneva, K. Müllen, S. Trapani, D. Beljonne, *Adv. Funct. Mater.* **2008**, *18*, 3947–3955; c) H. Frauenrath, E. Jahnke, *Chem. Eur. J.* **2008**, *14*, 2942–2955; d) E.-K. Schillinger, E. Mena-Osteritz, J. Hentschel, H. G. Börner, P. Bäuerle, *Adv. Mater.* **2009**, *21*, 1562–1567; e) T. Seki, A. Asano, S. Seki, Y. Kikkawa, H. Murayama, T. Karatsu, A. Kitamura, S. Yagai, *Chem. Eur. J.* **2011**, *17*, 3598–3608; f) R. J. Kumar, J. M. MacDonald, Th. B. Singh, L. J. Waddington, A. B. Holmes, *J. Am. Chem. Soc.* **2011**, *133*, 8564–8573; g) Y. Sun, L. Jiang, K. C. Schuermann, W. Adriaens, L. Zhang, F. Y. C. Boey, L. De Cola, L. Brunsveld, X. Chen, *Chem. Eur. J.* **2011**, *17*, 4746–4749; h) J. K. Gallaher, E. J. Aitken, R. A. Keyzers, J. M. Hodgkiss, *Chem. Commun.* **2012**, *48*, 7961–7963; i) R. J. Swanekamp, J. T. M. DiMaio, C. J. Bowerman, B. L. Nilsson, *J. Am. Chem. Soc.* **2012**, *134*, 5556–5559; j) L. Tian, R. Szilluweit, R. Marty, L. Bertschi, M. Zerson, E.-Ch. Spitzner, R. Magerled, H. Frauenrath, *Chem. Sci.* **2012**, *3*, 1512–1521; k) E. Orentas, M. Lista, N.-T. Lin, N. Sakai, S. Matile, *Nat. Chem.* **2012**, *4*, 746–750; l) R. Marty, R. Szilluweit, A. Sánchez-Ferrer, S. Bolisetty, J. Adamcik, R. Mezzenga, E.-C. Spitzner, M. Feifer, S. N. Steinmann, C. Corminboeuf, H. Frauenrath, *ACS Nano* **2013**, *7*, 8498–8508; m) D. Ivnitski, M. Amit, B. Rubinov, R. Cohen-Luria, N. Ashkenasy, G. Ashkenasy, *Chem. Commun.* **2014**, *50*, 6733–6736; n) R. Marty, R. Nigon, D. Leite, H. Frauenrath, *J. Am. Chem. Soc.* **2014**, *136*, 3919–3927.
- [5] Z. Chen, U. Baumeister, C. Tschierske, F. Würthner, *Chem. Eur. J.* **2007**, *13*, 450–465.
- [6] a) M. Kümin, L. S. Sonntag, H. Wennemers, *J. Am. Chem. Soc.* **2007**, *129*, 466–467.
- [7] For examples, see: a) D. G. McCafferty, D. A. Friesen, E. Danielson, C. G. Wall, M. J. Saderholm, B. W. Erickson, T. J. Meyer, *Proc. Natl. Acad. Sci. USA* **1996**, *93*, 8200–8204; b) K. M. Bonger, V. V. Kapoerhan, G. M. Grotenberg, C. J. Van Koppen, C. M. Timmers, G. A. van de Marel, H. S. Overkleef, *Org. Biomol. Chem.* **2010**, *8*, 1881–1884; c) G. Upert, F. Bouillière, H. Wennemers, *Angew. Chem. Int. Ed.* **2012**, *51*, 4231–4234; *Angew. Chem.* **2012**, *124*, 4307–4310; <lit d> C. Kroll, R. Mansi, F. Braun, S. Dobitz, H. R. Maecke, H. Wennemers, *J. Am. Chem. Soc.* **2013**, *135*, 16793–16796; e) D. Ma, S. E. Bettis, K. Hanson, M. Minakova, L. Alibabaei, W. Fondrie, D. M. Ryan, G. A. Papoian, T. J. Meyer, M. L. Waters, J. M. Papanikolas, *J. Am. Chem. Soc.* **2013**, *135*, 5250–5253.
- [8] a) C. W. Tornøe, C. Christensen, M. J. Meldal, *J. Org. Chem.* **2002**, *67*, 3057–3064; b) V. V. Rostovtsev, L. G. Green, V. V. Fokin, K. B. Sharpless, *Angew. Chem. Int. Ed.* **2002**, *41*, 2596–2599; *Angew. Chem.* **2002**, *114*, 2708–2711.
- [9] For details, see the Supporting Information.
- [10] F. Würthner, T. E. Kaiser, C. R. Saha-Möller, *Angew. Chem. Int. Ed.* **2011**, *50*, 3376–3410; *Angew. Chem.* **2011**, *123*, 3436–3473.
- [11] a) K. Koynov, H.-J. Butt, *Curr. Opin. Colloid Interface Sci.* **2012**, *17*, 377–387; b) T. B. Bonne, K. Ludtke, R. Jordan, P. Stepanek, C. M. Papadakis, *Colloid Polym. Sci.* **2004**, *282*, 833–843; Erratum: T. B. Bonne, K. Ludtke, R. Jordan, P. Stepanek, C. M. Papadakis, *Colloid Polym. Sci.* **2004**, *282*, 1425.
- [12] At the lowest examined concentration of 1 nM, none of the three compounds formed aggregates. This allowed for the determination of the hydrodynamic diameters of the individual oligoproline–PMI conjugates. Diameters of ca. 2.1 nm, ca. 2.4 nm, and ca. 3.2 nm were found for **1Sa**, **1Sb**, and **1Sc**, respectively, which correspond well with the expected effective sizes of the individual molecules (Ref. [9]).
- [13] Control experiments with non-conjugated azido functionalized oligoprolines and alkynylated PMI **A** revealed that the individual building blocks do not form such supramolecular assemblies (Ref. [9]), which corroborated that oligoprolines direct the formation of the well-defined nanostructured architectures.
- [14] The molecular dimensions of the conjugates were estimated based on a crystal structure of a related chromophore: P. D. Frischmann, Frank Würthner, *Org. Lett.* **2013**, *15*, 4674–4677, on the model of an oligoproline PPII-helix with Azp residues in every third position: M. Kuemin, S. Schweizer, C. Ochsenfeld, H. Wennemers, *J. Am. Chem. Soc.* **2009**, *131*, 15474–15482 that was based on the power diffractogram of oligoprolines: P. M. Cowan, S. McGavin, *Nature* **1955**, *176*, 501–503, and on the computer generated model of triazole functionalized chromophore **A** (Ref. [9]).
- [15] M. A. Hyatt, S. A. Miller, *Negative Staining*, McGraw Hill, **1990**.
- [16] “Exciton Chirality Method: Principles and Applications”: N. Berova, K. Nakanishi in *Circular Dichroism: Principles and Applications* (Eds.: N. Berova, K. Nakanishi, R. Woody), Wiley-VCH, Weinheim **2000**, pp. 337–382.